RADIATION RESEARCH **181**, 324–334 (2014)
0033-7587/14 $15.00

DOI: 10.1667/RR13452.1

Radiation-Induced Alterations in Mitochondria of the Rat Heart

Vijayalakshmi Sridharan,[a,1] Nukhet Aykin-Burns,[a] Preeti Tripathi,[a] Kimberly J. Krager,[a] Sunil K. Sharma,[b] Eduardo G. Moros,[c] Peter M. Corry,[b] Grazyna Nowak,[d] Martin Hauer-Jensen[a,e] and Marjan Boerma[a]

[a] *University of Arkansas for Medical Sciences, Department of Pharmaceutical Sciences, Division of Radiation Health, Little Rock, Arkansas;* [b] *University of Arkansas for Medical Sciences, Department of Radiation Oncology, Little Rock, Arkansas;* [c] *Moffitt Cancer Center and Research Institute, Department of Radiation Oncology, Tampa, Florida;* [d] *University of Arkansas for Medical Sciences, Department of Pharmaceutical Sciences, Little Rock, Arkansas; and* [e] *Surgical Service, Central Arkansas Veterans Healthcare System, Little Rock, Arkansas*

Sridharan, V., Aykin-Burns, N., Tripathi, P., Krager, K. J., Sharma, S. K., Moros, E. G., Corry, P. M., Nowak, G., Hauer-Jensen, M. and Boerma, M. Radiation-Induced Alterations in the Mitochondria of the Rat Heart. *Radiat. Res.* 181, 324–334 (2014).

Radiation therapy for the treatment of thoracic cancers may be associated with radiation-induced heart disease (RIHD), especially in long-term cancer survivors. Mechanisms by which radiation causes heart disease are largely unknown. To identify potential long-term contributions of mitochondria in the development of radiation-induced heart disease, we examined the time course of effects of irradiation on cardiac mitochondria. In this study, Sprague-Dawley male rats received image-guided local X irradiation of the heart with a single dose ranging from 3–21 Gy. Two weeks after irradiation, left ventricular mitochondria were isolated to assess the dose-dependency of the mitochondrial permeability transition pore (mPTP) opening in a mitochondrial swelling assay. At time points from 6 h to 9 months after a cardiac dose of 21 Gy, the following analyses were performed: left ventricular Bax and Bcl-2 protein levels; apoptosis; mitochondrial inner membrane potential and mPTP opening; mitochondrial mass and expression of mitophagy mediators Parkin and PTEN induced putative kinase-1 (PINK-1); mitochondrial respiration and protein levels of succinate dehydrogenase A (SDHA); and the 70 kDa subunit of complex II. Local heart irradiation caused a prolonged increase in Bax/Bcl-2 ratio and induced apoptosis between 6 h and 2 weeks. The mitochondrial membrane potential was reduced until 2 weeks, and the calcium-induced mPTP opening was increased from 6 h up to 9 months. An increased mitochondrial mass together with unaltered levels of Parkin suggested that mitophagy did not occur. Lastly, we detected a significant decrease in succinate-driven state 2 respiration in isolated mitochondria from 2 weeks up to 9 months after irradiation, coinciding with reduced mitochondrial levels of succinate dehydrogenase A. Our results suggest that local heart irradiation induces long-term changes in cardiac mitochondrial membrane functions, levels of SDH and state 2 respiration. At any time after exposure to radiation, cardiac mitochondria are more prone to mPTP opening. Future studies will determine whether this makes the heart more susceptible to secondary stressors such as calcium overload or ischemia/reperfusion.

INTRODUCTION

Radiotherapy of the thoracic region may lead to radiation exposure of the heart, despite recent advances in radiation delivery and planning techniques. Radiation-induced heart disease (RIHD) is a prominent and serious side effect of radiation exposure to the heart. RIHD is progressive, and clinical manifestations such as conduction abnormalities, injury to valves, pericardial and myocardial fibrosis and accelerated atherosclerosis take several years to decades to present (*1*, *2*). Currently, besides attempts to reduce cardiac radiation exposure during therapy, no method or approach for minimizing, preventing or reversing RIHD is available. Therefore, preclinical studies are necessary to unravel mechanisms that lead to the development of RIHD and help identify possible targets for intervention.

The heart demands high amounts of adenosine triphosphate (ATP) for its function and therefore relies heavily on its mitochondria (*3*). Hence, cardiomyocytes contain large numbers of mitochondria, which couple respiration with oxidative phosphorylation to generate ATP (*4–6*). Moreover, mitochondria are also involved in the maintenance of intracellular ion concentrations and the production and removal of reactive oxygen species (ROS). Furthermore, mitochondria play an important role in the regulation of several cellular functions, including stress responses, cell death and metabolic processes such as gluconeogenesis, β-oxidation and ketogenesis (*7*, *8*). Therefore, regulation of the various aspects of mitochondrial function is of high importance for the normal function of the heart.

Editor's note. The online version of this article (DOI: 10.1667/RR13452.1) contains supplementary information that is available to all authorized users.

[1] Address for correspondence: Division of Radiation Health, Department of Pharmaceutical Sciences, University of Arkansas for Medical Sciences, 4301 West Markham, Slot 522-10, Little Rock, AR 72205; e-mail: vmohanseenivasan@uams.edu.

Development of cardiovascular diseases is directly linked with impaired oxidative metabolism of mitochondria (*9–11*). In addition, mitochondria are sensitive to radiation and become a direct target of radiation damage within hours after exposure (*12*). Studies have shown that local heart irradiation can cause morphological damage in cardiac mitochondria (*13*, *14*), and nontransient mitochondrial functional alterations including impairment of the respiratory chain and increased protein oxidation (*15*, *16*). Irradiation has also been shown to increase the mitochondrial mass of certain cells in culture (*17–19*).

The main goal of our study was to investigate the time course of local heart irradiation-induced changes in cardiac mitochondria by examining Bax and Bcl2 levels, apoptosis, mitochondrial membrane potential, mitochondrial permeability transition pore (mPTP) opening and respiration.

MATERIALS AND METHODS

Animal Model of Local Heart Irradiation

All procedures in this study were approved by the Institutional Animal Care and Use Committee of the University of Arkansas for Medical Sciences. Male Sprague-Dawley rats were obtained from Harlan Laboratories and maintained in our Division of Laboratory Animal Medicine on a 12:12 light-to-dark cycle with free access to food and water. At a weight of 250–290 g rats received local heart irradiation with the small animal conformal radiation therapy device (SACRTD) developed at our institution. The SACRTD consists of a 225kVp X-ray source (GE Isovolt Titan 225, GE Sensing and Inspection Technologies, Billerica, MA) mounted on a custom made ''gantry'', a stage mounted on a robotic arm for positioning (Viper™ s650, Adept Technology, Pleasanton, CA) and a digital X-ray detector (XRD 0820 CM3, PerkinElmer, Waltham, MA). A brass and aluminum collimating assembly attached to the X-ray tube produced a field of 19 mm diameter at the isocenter (*20*).

Dosimetry was performed as described previously (*21*). In short, the dose rate at the isocenter was measured using a PinPoint® ion chamber (PTW N301013, PTW, Brooklyn, NY; ADCL calibrated for 225 kV), following the TG-61 protocol of the American Association of Physicists in Medicine (*22*). In addition, dosimetry was performed with Gafchromic® EBT-2 films (Ashland Specialty Ingredients, Wilmington, DE) that were calibrated with a Gamma Knife (Co-60) system (Elekta AB, Stockholm, Sweden) and analyzed as described previously (*23*). To measure relative depth dose, 11 pieces of film were placed in between 11 slabs of solid water phantom each 5 mm thick. The film on the top of the phantom was kept at the isocenter, normal to the beam direction and exposed to 5 Gy (225 kV, 13 mA).

For local heart irradiation, rats were anesthetized with 3% isoflurane and placed vertically in a cylindrical Plexiglas holder that was cut out such that no Plexiglas material was between the radiation beam and the chest. The heart was exposed in three 19 mm diameter fields (anterior-posterior and two lateral fields), given immediately after each other to a total dose of 3, 9 or 21 Gy (225 kV, 13 mA, 0.5 mm Cu-filtration, resulting in 1.92 Gy/min at 1 cm tissue depth). Before each exposure, the location of the heart was verified with the X-ray detector (70 kV, 5 mA, <1 cGy) and if necessary, the position of the rat was adjusted with the use of the robotic arm to place the heart in the middle of the radiation field. Rats were sacrificed at 2, 6 and 24 h, 4 days, 2 weeks, 10 weeks, 6 and 9 months after irradiation ($n = 3–6$ at each time point) or sham treatment ($n = 3–6$ at each time point) and hearts were collected for analysis.

Isolation of Mitochondria from Rat Hearts

Rats were anesthetized with 3% isoflurane, the heart was isolated and the left ventricle was immediately used for the isolation of mitochondria. The left ventricular tissue (180–200 mg) was minced and homogenized in 10 mL of a 10 m*M* Hepes pH 7.4 media containing 225 m*M* mannitol, 75 m*M* sucrose and 0.1 m*M* EGTA, using a mechanical Potter-Elvehjem homogenizer (Lab-Stirrer LR400C, Yamato Scientific America, Santa Clara, CA) (30 strokes at 100 rpm and 15 strokes at 125 rpm), with a Teflon® pestle. The homogenate was divided into 5 microcentrifuge tubes and centrifuged at 700*g* for 10 min at 4°C. The supernatant was removed and centrifuged at 12,500*g* for 30 min to obtain the mitochondrial pellet. This pellet was resuspended in a 10 m*M* Hepes pH 7.4 containing 395 m*M* sucrose and 0.1 m*M* EGTA, washed twice and immediately analyzed.

Mitochondrial Swelling Assay and Mitochondrial Membrane Potential

The mPTP opening was assessed by measuring calcium-induced swelling of freshly isolated mitochondria, indicated by a decrease in absorbance at 540 nm. This mitochondrial swelling assay was based on a method described previously (*24*). Briefly, isolated mitochondria were resuspended in swelling buffer pH 7.4 containing 120 m*M* KCl, 10 m*M* Tris HCl and 5 m*M* KH_2PO_4 to a final concentration of 150 μg/mL, and immediately exposed to vehicle, 250 μ*M* $CaCl_2$ or 250 μ*M* $CaCl_2$ in combination with 2 μ*M* cyclosporin A (CsA) as an inhibitor of mPTP opening. Optical density at 540 nm (OD540) was measured with a Synergy 4 microplate reader (BioTek), immediately before the assay and every 2 min thereafter for a total of 20 min.

Mitochondrial membrane potential was assessed with tetramethylrhodamine methyl ester (TMRM). TMRM is a cationic dye that accumulates in mitochondria in proportion to the mitochondrial membrane potential. Freshly isolated mitochondria were resuspended in a 10 m*M* Hepes pH 7.4 containing 395 m*M* sucrose and 0.1 m*M* EGTA, loaded with 50 or 200 n*M* TMRM, and incubated at room temperature for 15 min. Mitochondria were centrifuged at 14,000 rpm for 3 min to remove excess TMRM. The mitochondrial pellets were resuspended in 200 μl of 10 m*M* Hepes buffer pH 7.4 containing 395 m*M* sucrose and 0.1 m*M* EGTA and the fluorescence intensity was determined at 590 nm in a Synergy 4 microplate reader (BioTek).

TMRM fluorescence was normalized to mitochondrial protein content as measured with a bicinchoninic assay (BCA, Pierce). To correct for possible differences in TMRM uptake between mitochondrial isolations, each isolation included one sham-irradiated heart and one irradiated heart, and the normalized TMRM fluorescence of the mitochondria from the irradiated heart was calculated relative to the TMRM fluorescence of the mitochondria from the sham-irradiated heart in the same isolation.

Western Blots

Left ventricular tissue was homogenized in radioimmunoprecipitation assay (RIPA) buffer with freshly added inhibitor cocktails of proteases (10 μL/mL) and phosphatases (10 μL/mL, both Sigma-Aldrich, St. Louis, MO), centrifuged at 20,000*g* at 4°C for 15 min, and the supernatant was collected. Similarly, mitochondria pellets were lysed with RIPA buffer containing protease and phosphatase inhibitors for 30 min with intermittent vortexing. The lysates were centrifuged at 14,000 rpm for 10 min and the supernatants were collected. Amounts of protein were determined with a BCA protein assay (Pierce). A total of 50 μg protein was prepared in Laemmli sample buffer containing β-mercaptoethanol (1:20 vol/vol) and boiled for 2–3 min. Protein samples were separated either in Any kD™ Mini-Protean® polyacrylamide gels or 4–20% gradient polyacrylamide gels (Bio-Rad, Hercules, CA) at 100 Volts and transferred to PVDF membranes at 20 Volts overnight at 4°C.

Nonspecific antibody binding was reduced by TBS containing 0.05% Tween-20 and 5% nonfat dry milk. Membranes were then incubated overnight with rabbit anti-Bax (1:1,000, Santa Cruz Biotechnology Inc., Dallas, TX), rabbit anti-Bcl2 (1:1,000, Santa Cruz Biotechnology Inc.), rabbit anti-Parkin (1:2,000 Santa Cruz Biotechnology Inc.), rabbit anti-PTEN-induced kinase 1 (PINK-1, 1:2,000, Santa Cruz Biotechnology Inc.), mouse anti-succinate dehydrogenase A (SDHA) the 70 kDa subunit of complex II (1:60,000, Life Technologies, Grand Island, NY) all in TBS containing 5% nonfat dry milk and 0.1% Tween-20, followed by HRP conjugated mouse anti-rabbit or goat anti-mouse antibodies, 1:5,000 for 1 h (Cell Signaling Technology Inc., Danvers, MA). Protein loading was visualized by incubating membranes in mouse anti-GAPDH (1:20,000, Santa Cruz Biotechnology Inc.) or mouse anti-F0-F1 ATPase (1:60,000, Life Technologies) for 1 h followed by HRP-conjugated goat anti-mouse, 1:20,000 (Jackson ImmunoResearch Laboratories Inc., Westgrove, PA). Antibody binding was visualized with ECL™ Plus Western Blotting Detection reagent (GE Healthcare Life Sciences, Pittsburgh, PA) on CL-Xposure Film (Thermo Scientific, Pittsburgh, PA). Films were scanned using an AlphaImager® gel documentation system (ProteinSimple, Santa Clara, CA) and protein bands were quantified with the public domain software ImageJ (http://rsbweb.nih.gov/ij/).

Measurement of Mitochondrial Respiration by XF96 Extracellular Flux Analyzer

Oxygen consumption rate (OCR) of isolated mitochondria was measured in an XF96 Extracellular Flux Analyzer (Seahorse Bioscience, North Bellerica, MA) based on a previously described method (*25*) with modifications for the XF96 instrument. Rats were anesthetized with 3% isoflurane, the heart was isolated and the left ventricle was immediately used for the isolation of mitochondria. Left ventricular tissue (180–200 mg) was minced and homogenized in 10 mL of a 10 m*M* Hepes buffer pH 7.4 containing 225 m*M* mannitol, 75 m*M* sucrose, 1 m*M* EGTA and 0.5% (w/v) fatty acid-free BSA using a mechanical Potter-Elvehjem homogenizer (Lab-Stirrer LR400C, Yamato), 30 strokes at 100 rpm and 15 strokes at 125 rpm with a Teflon® pestle. The homogenate was divided into 5 microcentrifuge tubes and centrifuged at 700*g* for 10 min at 4°C. The supernatant was removed and centrifuged at 12,500*g* for 30 min to obtain the mitochondrial pellet. This pellet was resuspended in 2 m*M* Hepes buffer pH 7.4 containing 225 m*M* mannitol, 75 m*M* sucrose, 10 m*M* KH_2PO_4, 5 m*M* $MgCl_2$, 1 m*M* EGTA and 0.2% (w/v) fatty acid-free BSA (mitochondrial suspension buffer, pH 7.4) washed twice, and the pellet was weighed and resuspended in the same buffer to make a final concentration of 50 mg mitochondria/ml.

A total of 20 µl mitochondrial suspension containing different concentrations ranging from 10–50 µg mitochondria/ml in mitochondrial suspension buffer with 10 m*M* succinic acid and 0.2 µ*M* rotenone, or in mitochondrial suspension buffer with 5 m*M* glutamic acid and 5 m*M* malic acid (all Agros Organics) was added to the appropriate wells of an Seahorse XF96 microplate (8 wells for each mitochondrial mass). The plate was centrifuged at 2,000*g* for 20 min at 4°C to attach the mitochondria to the bottom of the plate. The mitochondria were viewed briefly under a microscope to ensure consistent adherence to the wells, and 140 µl of the succinate or glutamate-malate buffer was added to the corresponding wells. The plate was then placed at 37°C for 10 min to allow it to warm before transfer to the XF96 instrument. Four baseline (state 2 respiration) measurements were acquired before injection of mitochondrial inhibitors or uncouplers. Readings were taken after sequential addition of ADP (5 m*M*, state 3 respiration), oligomycin (10 µ*M*, state 4 respiration) and the uncouplers: p-trifluoromethoxyphenylhydrazone (FCCP) (4 µ*M*) and antimycin A (10 µ*M*). For each well of the plate, OCR was calculated with the Seahorse XF96 software and was normalized for the mitochondrial mass. To correct for possible differences between mitochondrial isolations, each XF96 plate contained mitochondria from one sham-irradiated heart and one irradiated heart, and within each plate the OCR of the irradiated mitochondria was calculated relative to the OCR of the sham-irradiated mitochondria.

Histology

Hearts were fixed in formalin, embedded in paraffin and 5 µ*M* longitudinal sections were used for determination of apoptotic nuclei. The CardioTACS™ Kit (Trevigen Inc., Gaithersburg, MD), which is based on DNA end-labeling with terminal deoxynucleotidyl transferase, was used according to the manufacturer's instructions. Stained sections were examined with an Axioskop transmitted light microscope (Carl Zeiss, Munich, Germany) and the apoptotic nuclei in the ventricles of each heart section were counted.

Statistical Analysis

Data were evaluated with the software package NCSS 8 (NCSS LLC, Kaysville, UT). Data were analyzed with two-way ANOVA or repeated measures ANOVA (mitochondrial swelling assay), followed by Newman-Keuls individual comparisons. The criterion for significance was $P < 0.05$.

RESULTS

Local Heart Irradiation Caused a Prolonged Upregulation of Bax and Increased Apoptosis at Early Time Points

First, we studied the protein levels of Bax and Bcl2 in total left ventricular lysates. Radiation caused a significant increase in the expression of Bax at time points from 6 h to 2 weeks after irradiation and an increase in the Bax/Bcl2 ratio from 6 h to 6 months after irradiation (Fig. 1A). To verify that increased levels of Bax coincided with mitochondrial translocation of Bax, Bax and Bcl-2 levels were examined in mitochondria isolated at 2 weeks after irradiation (Fig. 1B). Mitochondrial Bax was significantly upregulated, leading to an increased Bax/Bcl2 ratio. Since increased mitochondrial Bax can initiate apoptotic cell death, we examined whether there was evidence of apoptosis in the left ventricles of irradiated hearts. A significant increase in the number of apoptotic nuclei was found at 6 and 24 h and 2 weeks after irradiation (Table 1 and Supplementary Fig. S3; http://dx.doi.org/10.1667/RR13452.1.S1).

Local Heart Irradiation Caused Early Alterations in Mitochondrial Membrane Potential and an Enhanced and Prolonged mPTP Opening

The effects of local heart irradiation on mitochondrial membrane potential were assessed by mitochondrial uptake of TMRM. Reduced uptake of TMRM at 6 h and 2 weeks after irradiation indicated a reduced mitochondrial membrane potential (Fig. 2A). Swelling assays were performed with mitochondria isolated from left ventricles of sham and irradiated hearts, to examine the opening of mPTP in response to calcium. Enhanced mitochondrial swelling in response to calcium was observed from 2 weeks to 9

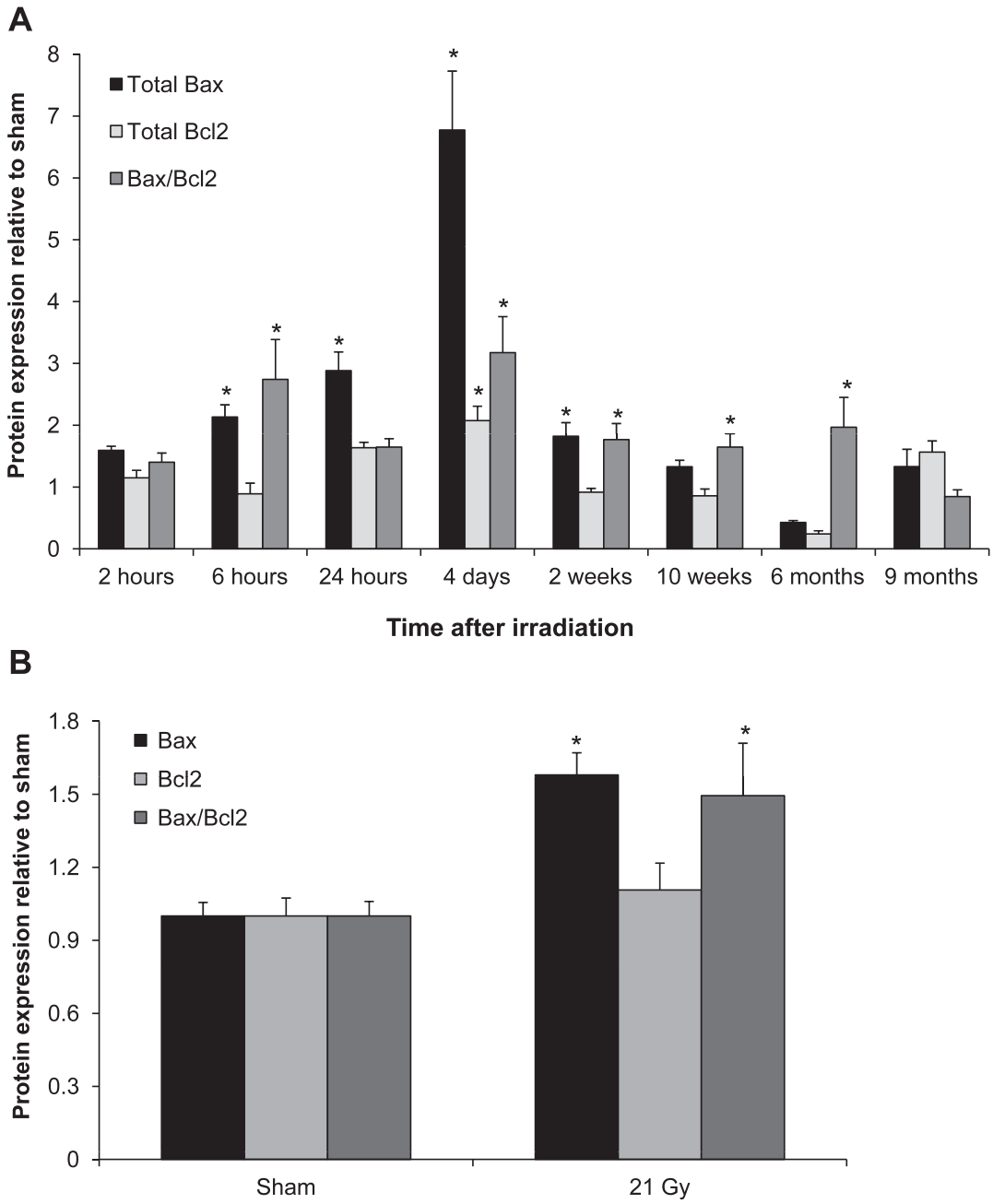

FIG. 1. Effects of local heart irradiation on the protein expression of Bax and Bcl2. Panel A: Radiation caused an increase in left ventricular Bax levels between 6 h and 2 weeks and an increase in Bax/Bcl2 ratios between 6 h and 6 months after irradiation. Panel B: Mitochondrial Bax levels and Bax/Bcl2 ratio were increased at 2 weeks after irradiation. Average ± sem n = 5–6. *$P < 0.05$ when compared to sham-irradiated control.

months after irradiation (Fig. 2B and Supplementary Fig. S1; http://dx.doi.org/10.1667/RR13452.1.S1). Mitochondrial swelling was inhibited by CsA, indicating that it was caused by mPTP opening. To assess dose dependency of radiation-induced susceptibility to mPTP opening, the effects of 3 and 9 Gy were also examined at 2 weeks after local heart irradiation. Calcium-induced mitochondrial swelling was dose dependent, with a statistically significant effect of 9 and 21 Gy (Supplementary Fig. S4; http://dx.doi.org/10.1667/RR13452.1.S1).

Local Heart Irradiation did not Cause Indications of Mitophagy

Cardiac diseases may be associated with increased mitophagy, a form of autophagic degradation of damaged mitochondria. While mitochondrial levels of the mitophagy

TABLE 1
Numbers of Apoptotic Nuclei in the Ventricles of Rat Hearts at Different Time Points after Irradiation (Average ± Sem, n = 3)

Time after irradiation	Number of apoptotic nuclei	
	Sham	21 Gy
2 h	175 ± 38	204 ± 29
6 h	175 ± 38	1301 ± 91[a]
24 h	175 ± 38	755 ± 83[a]
4 days	175 ± 38	211 ± 61
2 weeks	60 ± 19	132 ± 23[a]
6 months	15 ± 4	15 ± 2

Note. Representative images of the CardioTACS™ stainings are shown in Supplementary Fig. S3 (http://dx.doi.org/10.1667/RR13452.1.S1).

[a] $P < 0.05$ when compared to sham-irradiated control.

mediator PINK-1 were significantly increased at 2 weeks and reduced at 10 weeks after irradiation, mitochondrial protein levels of Parkin, which is recruited by PINK-1 to initiate mitophagy, did not change with radiation (Fig. 3A and Table 2). Moreover, at all time points of investigation the mitochondrial isolation resulted in a larger mass of mitochondria from irradiated hearts (Fig. 3B).

Local Heart Irradiation Caused Changes in Mitochondrial Respiration

A representative graph of the OCR measurements is shown in Supplementary Fig. S2 (http://dx.doi.org/10.1667/RR13452.1.S1). Figure 4A shows the OCR when succinate was provided as a substrate for mitochondrial complex II and rotenone as an inhibitor of complex I. Basal (state 2) OCR was significantly reduced in mitochondria isolated from irradiated hearts at all time points of investigation, while ADP-driven (state 3) OCR was not significantly altered by radiation. The OCR in the presence of ATP synthase inhibitor oligomycin (state 4 respiration), which reflects the amount of proton leak across the inner mitochondrial membrane, was reduced at 2 weeks after irradiation, while the respiratory control ratio (RCR, state 3/state 4) did not change at any of the time points (data not shown). Lastly, no differences in uncoupled respiration (maximal respiration capacity) were found between mitochondria isolated from sham-irradiated and irradiated hearts (data not shown). Interestingly, we also observed reduced protein levels of SDHA, the 70 kDa subunit of the respiratory chain component complex II in both total left ventricular lysates and mitochondrial lysates at 2 and 10 weeks and 6 months after local heart irradiation (Figs. 4B and C).

In glutamate-malate buffer, which provides glutamate and malate as substrates for mitochondrial complex I, no significant effects of radiation were observed on basal respiration, state 3 respiration, state 4 respiration, RCR or uncoupled OCR (data not shown).

DISCUSSION

Exposure to ionizing radiation is a risk factor for the development of cardiovascular diseases. The current study used a rat model of local heart irradiation to investigate the time course of radiation-induced changes in cardiac mitochondrial membrane characteristics and respiration. Although this is a predominantly observational study, to our knowledge it is the first to assess an extensive time course of cardiac mitochondrial alterations and to show increased susceptibility to mitochondrial permeability transition (MPT) in mitochondria from the irradiated heart.

Bax is one of the important proapoptotic proteins of the Bcl-2 family (*26–29*). Under normal conditions, Bax is homogenously distributed in the cytoplasm. However, under conditions of stress, increased expression and activation of Bax leads to its translocation and insertion into the outer mitochondrial membrane (*30–33*). Translocation of Bax to the outer mitochondrial membrane is one of the prerequisites for MPT and mitochondrial membrane depolarization that may lead to the onset of apoptosis (*34*, *35*). In our study, local heart irradiation caused an increase in total left ventricular Bax levels at earlier time points, a prolonged increase in Bax/Bcl2 ratios and increased mitochondrial Bax level (content), prompting us to examine apoptosis. A significant increase in the number of apoptotic nuclei was observed at early time points only: 6 and 24 h and 2 weeks after irradiation, coinciding with the increased left ventricular expression of Bax. These results are in accordance with radiation-induced apoptosis in other organs, showing increased numbers of apoptotic cells from 6 h to several weeks after irradiation (*36–38*). However, a recent study has demonstrated the presence of cleaved–caspase 3 at 13 months after local heart irradiation in the rat (*14*). Hence, we cannot exclude that apoptosis may occur again at time points beyond 9 months in our rat model of local heart irradiation. Interestingly, a large part of the heart consists of highly differentiated cardiomyocytes that may not likely undergo early (premitotic) apoptosis. Also, a previous study has shown that cardiac endothelial cells undergo a late mitotic death after irradiation (*39*). Therefore, cardiac endothelial cells may not have contributed to the early increases in apoptotic cells in our study. Future experiments may elucidate the exact nature of the apoptotic cells in the irradiated heart.

Translocation and insertion of Bax into the mitochondrial membrane has been shown to accelerate the opening of the mitochondrial voltage-dependent anion channel leading to increased mitochondrial membrane permeability and loss of mitochondrial membrane potential (*40*). MPT and loss of mitochondrial membrane potential are important mechanisms of mitochondrial dysfunction and are involved in the pathogenesis of many cardiovascular diseases (*26*, *41*, *42*). MPT is a process characterized by increased swelling of mitochondria, depolarization of the mitochondrial membrane and the uncoupling of oxidative phosphorylation (*43*).

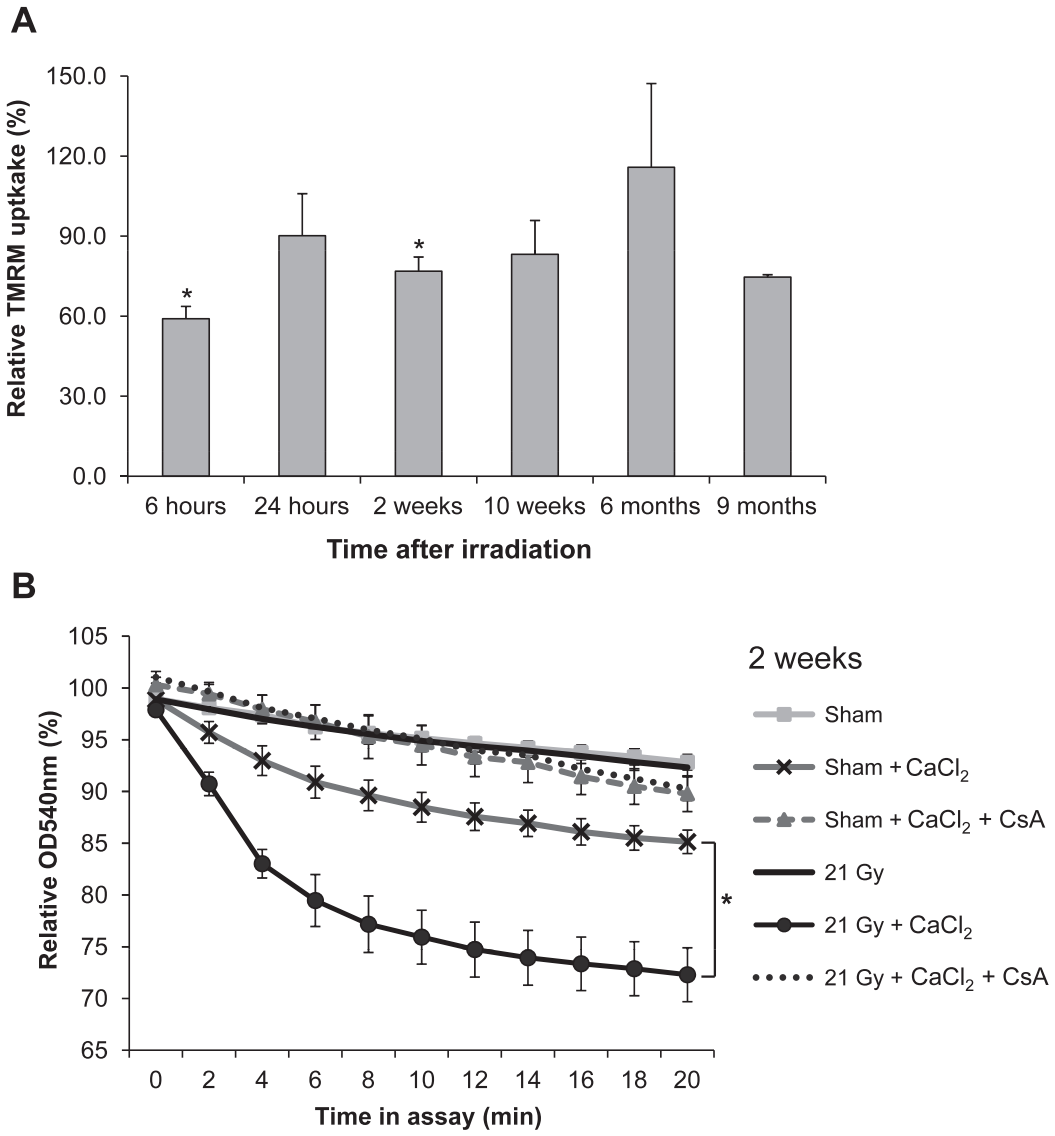

FIG. 2. Effects of local heart irradiation on mitochondrial membrane properties. Panel A: Mitochondrial membrane potential, as assessed by uptake of TMRM in isolated mitochondria, was significantly reduced at 6 h and 2 weeks after irradiation. Isolated mitochondria were incubated with TMRM, washed and the mitochondrial fluorescence was normalized to mitochondrial protein content. These normalized values for TMRM fluorescence of mitochondria isolated from irradiated hearts were calculated relative to the TMRM fluorescence of mitochondria isolated from sham-irradiated hearts. Panel B: Representative figure of the results of the swelling assay with mitochondria isolated at 2 weeks after irradiation. Swelling was assessed as a reduction in the OD540 nm of mitochondrial suspensions, relative to the OD540 nm of the same mitochondrial samples immediately before the start of the assay. Swelling was inhibited by CsA, indicating that swelling was due to mPTP opening. Swelling assays of other time points are shown in Supplementary Fig. S1 (http://dx.doi.org/10.1667/RR13452.1.S1). Average ± sem, n = 5–6. $*P < 0.05$ when compared to sham-irradiated control.

A variety of stimuli such as calcium influx into mitochondria, inorganic phosphate, ROS and other oxidant chemicals can induce the onset of MPT (*42*, *44–46*). The increase in the inner mitochondrial membrane permeability is mediated by the opening of the mPTP, a nonspecific channel that spans both inner and outer mitochondrial membranes or by channels formed by insertion of Bax (*47*). mPTP opening can be assessed with a mitochondrial swelling assay, in which mitochondrial swelling in response to exogenous calcium is an indicator of mPTP opening. In our study, mitochondria isolated from irradiated hearts were more prone to swelling in response to calcium. Interestingly, this effect was observed at all time points of investigation (6 h to 9 months) and showed a dose dependency (3–21 Gy). However, mitochondria were isolated from whole left ventricular tissue and we therefore cannot be certain of the cellular origin of the mitochondria. Nonetheless, since cardiomyocytes occupy approximately 75% of the normal

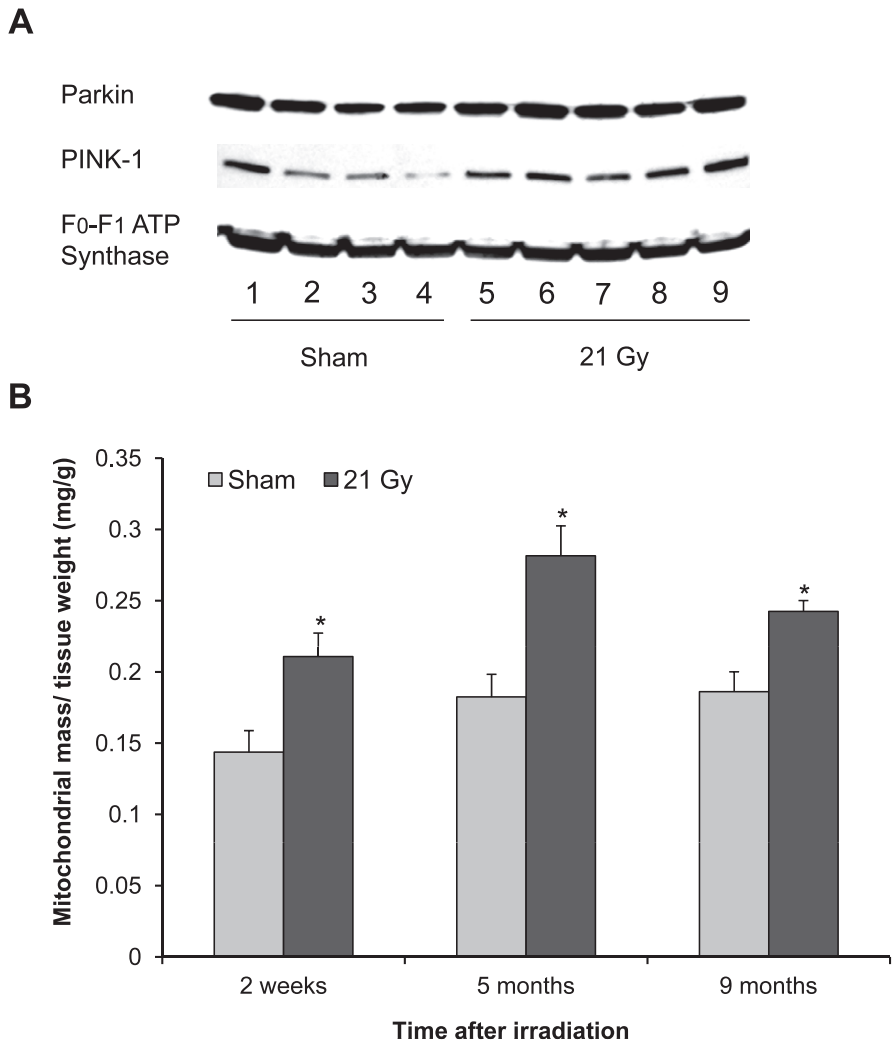

FIG. 3. Effects of local heart irradiation on mitophagy mediators and mitochondrial mass. Panel A: Representative immunoblot showing protein levels of mitophagy mediators in mitochondrial lysates at 6 months after sham-irradiation (lanes 1–4) or irradiation (lanes 5–9). Data of all time points are shown in Table 2. Panel B: The mitochondrial isolation resulted in a larger mass of mitochondria from irradiated hearts. Average ± sem, n = 4–5. *$P < 0.05$ when compared to sham-irradiated control.

myocardial tissue volume and are highly enriched in mitochondria, we assume that most of the isolated mitochondria in this study originated from cardiomyocytes. Therefore, our results suggest that cardiomyocytes in irradiated hearts are more susceptible to MPT in response to secondary stressors such as deregulation of calcium homeostasis or ischemia/reperfusion (*48*, *49*).

Mitochondrial membrane integrity is important for cardiomyocyte survival and energy homeostasis. Loss of mitochondrial membrane potential is an important factor in determining the extent of damage sustained by mitochondria (*50*). In our study, even though we observed a prolonged and enhanced calcium-induced swelling in mitochondria isolated from irradiated hearts, we found decreased mitochondrial membrane potential at only 6 h and 2 weeks postirradiation. Previous studies have shown that depolarization of the mitochondrial membrane potential and MPT after clinical doses of ionizing radiation is reversible (*51*). Thus, it is unlikely that a significant number of mitochondria undergo MPT as a direct consequence of irradiation. However, our results suggest that ionizing

TABLE 2
Mitochondrial Levels of PINK-1 and Parkin at Different Time Points after Irradiation, as Measured with Western Blots (Average ± Sem, n = 4–5)

Time after irradiation	PINK-1		Parkin	
	Sham	21 Gy	Sham	21 Gy
24 h	0.98 ± 0.07	1.30 ± 0.32	1.60 ± 0.11	2.27 ± 0.23
2 weeks	1.31 ± 0.40	2.36 ± 0.22[a]	1.03 ± 0.12	0.95 ± 0.11
10 weeks	1.09 ± 0.25	0.41 ± 0.11[a]	2.98 ±0.39	2.27 ± 0.31
6 months	0.88 ± 0.06	1.29 ± 0.20	4.05 ± 0.29	5.25 ± 0.48

Note. F0-F1 ATP synthase was used as a loading control.
[a] $P < 0.05$ when compared to sham-irradiated control.

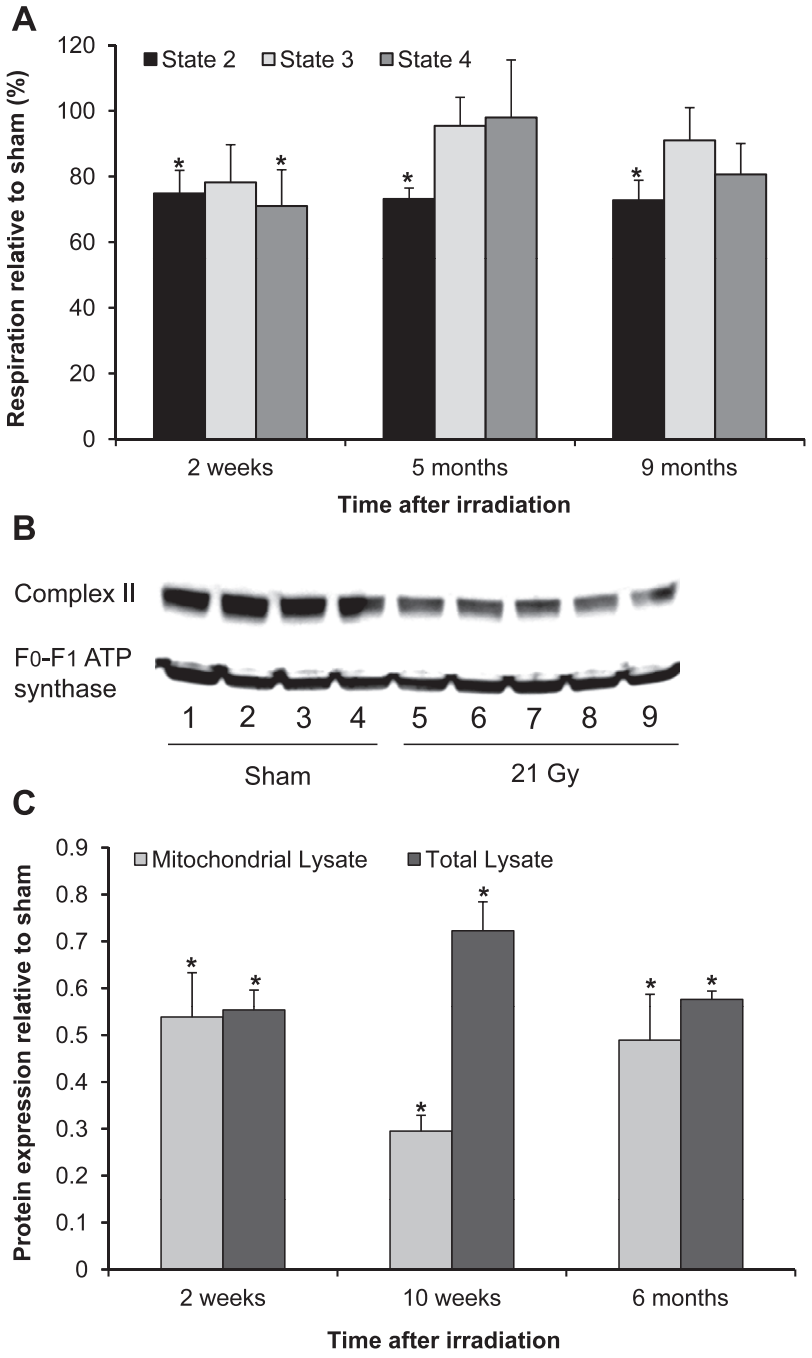

FIG. 4. Effects of local heart irradiation on mitochondrial respiration. Panel A: Mitochondria isolated from irradiated hearts showed reductions in succinate-dependent state 2 respiration relative to state 2 and respiration in mitochondria isolated from sham-irradiated hearts, no significant changes in state 3 respiration and reduced state 4 respiration at 2 weeks only. Panel B: Representative immunoblot of mitochondrial protein levels of SDHA, the 70 kDa subunit of respiratory complex II at 6 months after sham-irradiation (lanes 1–4) or irradiation (lanes 5–9); Panel C: At all time points, decreased state 2 respiration coincided with reduced mitochondrial protein levels of SDHA. Average ± sem, n = 4–6. *$P < 0.05$ when compared to sham-irradiated control.

radiation might induce transient changes in mitochondria, and that further events that may increase mitochondrial ROS or calcium overload may enhance the susceptibility for MPT in mitochondria in hearts that were previously exposed to radiation.

In our study, mitochondrial isolations resulted in a larger mass of mitochondria isolated from irradiated hearts compared to sham-irradiated hearts at all time points of investigation. Similarly, previous studies have reported an increased mitochondrial mass in cells in culture after

irradiation (*17*, *18*). Persistent injury to mitochondria may cause cells to increase their mitochondrial mass as a compensatory mechanism to maintain their levels of ATP from oxidative phosphorylation (*52–54*). The unaltered levels of mitophagy marker Parkin after irradiation in the present study suggest that mitophagy did not occur until 9 months after exposure to local heart irradiation. Further studies need to address whether mitochondrial biogenesis may be responsible for the increased mitochondrial mass observed after irradiation.

Measurement of oxygen consumption in mitochondria isolated from irradiated hearts demonstrated reduced basal (state 2) respiration in the presence of the complex II substrate succinate combined with the complex I inhibitor rotenone, from 2 weeks to 9 months after irradiation. State 2 OCR reflects the reduction in molecular oxygen in a sample of mitochondria in the absence of ATP production. State 2 OCR may be caused by an altered substrate transport into the mitochondria, partial uncoupling of the mitochondria, or the use of oxygen by other enzymes that are not involved in oxidative phosphorylation. However, these last two potential causes may not explain why we observed a change in state 2 OCR with the substrate succinate only, and not with the substrates glutamate and malate. State 3 OCR was not significantly reduced in mitochondria isolated from irradiated hearts, suggesting that the maximum respiratory capacity was not affected by radiation. In line with our observation, studies by Barjaktarovic *et al*. have also reported decreased succinate-driven state 2 OCR with no significant changes in state 3 respiration in mouse hearts at 4 and 40 weeks after local heart irradiation (*15*, *16*). In contrast, Franken *et al*. observed reduced state 3 respiration driven by the substrates succinate and β-hydroxybutyrate at different time points after local heart irradiation in the rat (*55*). However, the OCR was calculated per gram of left ventricular tissue, not correcting for the amount of mitochondria in the tissue.

In the current study, the reduced succinate-dependent respiration coincided with a significant reduction in the protein levels of SDHA both in mitochondrial lysates and in total lysates. Complex II plays a dual role in the Krebs cycle and mitochondrial respiration and has unique redox properties that differ from other mitochondrial dehydrogenases (*56*). Complex II acts as a major source of electrons for the production of ROS (*57*) and, together with ubiquinone, controls the superoxide generating activity of the respiratory chain in mitochondria (*58*). Future studies are needed to identify whether reduced mitochondrial levels of complex II are associated with the reduced state 2 OCR that we observed, or an altered production of intracellular ROS in the irradiated heart.

In conclusion, the current study has shown that local heart irradiation caused long-term changes in mitochondrial membrane functions, levels of SDHA and state 2 OCR. Future studies will be required to elucidate whether and how these radiation-induced mitochondrial changes may contribute to the development of RIHD, and make the heart more susceptible to secondary stressors due to the enhanced tendency of mPTP opening.

SUPPLEMENTARY INFORMATION

Supplementary Fig. S1. http://dx.doi.org/10.1667/RR13452.1.S1; Swelling assays with mitochondria isolated from the left ventricles of hearts at 6 h (panel A), 10 weeks (panel B), 6 months (panel C) and 9 months (panel D) after local heart irradiation. Swelling was assessed as mitochondrial optical density at 540 nm (OD540 nm) when in the assay, relative to their OD540 nm immediately before the start of the assay. Incubation of mitochondria from irradiated hearts with $CaCl_2$ caused swelling that was blocked by cyclosporin A (CsA), an inhibitor of transition pore opening. Average ± sem, n = 5–6. $*P < 0.05$ when compared to sham-irradiated control.

Supplementary Fig. S2. http://dx.doi.org/10.1667/RR13452.1.S1; Diagram of the measurements of oxygen consumption at state 2, state 3 and state 4 respiration.

Supplementary Fig. S3. http://dx.doi.org/10.1667/RR13452.1.S1; Panel A: Representative immunoblot showing protein levels of Bax and Bcl2 in left ventricular lysates at 6 months after sham-irradiation (lanes 1–6) or local heart irradiation (lanes 7–12). Panel B: Representative CardioTACS™ staining at 2 weeks after sham-irradiation, 20× magnification. Panel C: Representative CardioTACS staining at 2 weeks after local heart irradiation with 21 Gy, 20× magnification. Apoptotic nuclei are stained blue.

Supplementary Fig. S4. http://dx.doi.org/10.1667/RR13452.1.S1; Dose-dependent effect of radiation on the susceptibility of mPTP opening in mitochondria isolated from left ventricular samples at 2 weeks after local heart irradiation with a single dose of 3, 9 or 21 Gy. Average ± sem, n = 4. $*P < 0.05$ when compared to sham-irradiated control.

ACKNOWLEDGMENTS

This work was supported by the National Institutes of Health (CA148679, CA71382) and the American Cancer Society (RSG-10-125-01-CCE).

Received: June 28, 2013; accepted: November 4, 2013; published online: February 25, 2014

REFERENCES

1. Adams MJ, Hardenbergh PH, Constine LS, Lipshultz SE. Radiation-associated cardiovascular disease. Crit Rev Oncol Hematol 2003; 45:55–75.
2. Heidenreich PA, Hancock SL, Vagelos RH, Lee BK, Schnittger I. Diastolic dysfunction after mediastinal irradiation. Am Heart J 2005; 150:977–82.
3. Finck BN and Kelly DP. Peroxisome proliferator-activated receptor gamma coactivator-1 (PGC-1) regulatory cascade in cardiac physiology and disease. Circulation 2007; 115:2540–48.
4. Mitchell P. Coupling of phosphorylation to electron and hydrogen

transfer by a chemi-osmotic type of mechanism. Nature 1961; 191:144–8.

5. Fernie AR, Carrari F, Sweetlove LJ. Respiratory metabolism: glycolysis, the TCA cycle and mitochondrial electron transport. Curr Opin Plant Biol 2004; 7:254–61.
6. Reichert AS and Neupert W. Mitochondriomics or what makes us breathe. Trends Genet 2004; 20:555–62.
7. Galluzzi L, Kepp O, Trojel-Hansen C, Kroemer G. Mitochondrial control of cellular life, stress, and death. Circ Res 2012; 111:1198–1207.
8. Liesa M, Palacin M, Zorzano A. Mitochondrial dynamics in mammalian health and disease. Physiol Rev 2009; 89:799–845.
9. Ballinger SW. Mitochondrial dysfunction in cardiovascular disease. Free Radic Biol Med 2005; 38:1278–95.
10. Dhalla NS, Temsah RM, Netticadan T. Role of oxidative stress in cardiovascular diseases. J Hypertens 2000; 18:655–73.
11. Takano H, Zou Y, Hasegawa H, Akazawa H, Nagai T, Komuro I. Oxidative stress-induced signal transduction pathways in cardiac myocytes: involvement of ROS in heart diseases. Antioxid Redox Signal 2003; 5:789–94.
12. Azimzadeh O, Scherthan H, Sarioglu H, Barjaktarovic Z, Conrad M, Vogt A, et al. Rapid proteomic remodeling of cardiac tissue caused by total body ionizing radiation. Proteomics 2011; 11:3299–3311.
13. Cilliers GD, Harper IS, Lochner A. Radiation-induced changes in the ultrastructure and mechanical function of the rat heart. Radiother Oncol 1989; 16:311–26.
14. Ferreira-Machado SC, Salata C, Rocha NN, Correa AF, Corte-Real S, Peregrino AA, et al. Caspase-3 activation and increased procollagen type I in irradiated hearts. An Acad Bras Cienc 2013; 85:215–22.
15. Barjaktarovic Z, Schmaltz D, Shyla A, Azimzadeh O, Schulz S, Haagen J, et al. Radiation-induced signaling results in mitochondrial impairment in mouse heart at 4 weeks after exposure to X-rays. PLoS One 2011; 6:e27811.
16. Barjaktarovic Z, Shyla A, Azimzadeh O, Schulz S, Haagen J, Dorr W, et al. Ionising radiation induces persistent alterations in the cardiac mitochondrial function of C57BL/6 mice 40 weeks after local heart exposure. Radiother Oncol 2013; 106:404–10.
17. Dayal D, Martin SM, Owens KM, Aykin-Burns N, Zhu Y, Boominathan A, et al. Mitochondrial complex II dysfunction can contribute significantly to genomic instability after exposure to ionizing radiation. Radiat Res 2009; 172:737–45.
18. Nugent SM, Mothersill CE, Seymour C, McClean B, Lyng FM, Murphy JE. Increased mitochondrial mass in cells with functionally compromised mitochondria after exposure to both direct gamma radiation and bystander factors. Radiat Res 2007; 168:134–42.
19. Wang L, Kuwahara Y, Li L, Baba T, Shin RW, Ohkubo Y, et al. Analysis of common deletion (CD) and a novel deletion of mitochondrial DNA induced by ionizing radiation. Int J Radiat Biol 2007; 83:433–42.
20. Sharma S, Moros EG, Boerma M, Sridharan V, Han EY, Clarkson R, et al. A novel technique for image-guided local heart irradiation in the rat. TCRT Express 2013; 1:47–57.
21. Sridharan V, Tripathi P, Sharma SK, Moros EG, Corry P, Lieblong BJ, et al. Cardiac inflammation after local irradiation is influenced by the kallikrein-kinin system. Cancer Res 2012; 72:4984–92.
22. Ma CM, Coffey CW, DeWerd LA, Liu C, Nath R, Seltzer SM, et al. AAPM protocol for 40–300 kV x-ray beam dosimetry in radiotherapy and radiobiology. Med Phys 2001; 28:868–93.
23. Devic S, Seuntjens J, Sham E, Podgorsak EB, Schmidtlein CR, Kirov AS, et al. Precise radiochromic film dosimetry using a flat-bed document scanner. Med Phys 2005; 32:2245–53.
24. Maloyan A, Sanbe A, Osinska H, Westfall M, Robinson D, Imahashi K, et al. Mitochondrial dysfunction and apoptosis underlie the pathogenic process in alpha-B-crystallin desmin-related cardiomyopathy. Circulation 2005; 112:3451–61.
25. Rogers GW, Brand MD, Petrosyan S, Ashok D, Elorza AA, Ferrick DA, et al. High throughput microplate respiratory measurements using minimal quantities of isolated mitochondria. PLoS One 2011; 6:e21746.
26. Kroemer G, Galluzzi L, Brenner C. Mitochondrial membrane permeabilization in cell death. Physiol Rev 2007; 87:99–163.
27. Crow MT, Mani K, Nam YJ, Kitsis RN. The mitochondrial death pathway and cardiac myocyte apoptosis. Circ Res 2004; 95:957–70.
28. Gross A, McDonnell JM, Korsmeyer SJ. BCL-2 family members and the mitochondria in apoptosis. Genes Dev 1999; 13:1899–1911.
29. Sharpe JC, Arnoult D, Youle RJ. Control of mitochondrial permeability by Bcl-2 family members. Biochim Biophys Acta 2004; 1644:107–13.
30. An J, Li P, Li J, Dietz R, Donath S. ARC is a critical cardiomyocyte survival switch in doxorubicin cardiotoxicity. J Mol Med (Berl) 2009; 87:401–10.
31. Brady NR, Hamacher-Brady A, Gottlieb RA. Proapoptotic BCL-2 family members and mitochondrial dysfunction during ischemia/reperfusion injury, a study employing cardiac HL-1 cells and GFP biosensors. Biochim Biophys Acta 2006; 1757:667–78.
32. Capano M, Crompton M. Bax translocates to mitochondria of heart cells during simulated ischaemia: involvement of AMP-activated and p38 mitogen-activated protein kinases. Biochem J 2006; 395:57–64.
33. Gustafsson AB, Tsai JG, Logue SE, Crow MT, Gottlieb RA. Apoptosis repressor with caspase recruitment domain protects against cell death by interfering with Bax activation. J Biol Chem 2004; 279:21233–8.
34. Shimizu S, Narita M, Tsujimoto Y. Bcl-2 family proteins regulate the release of apoptogenic cytochrome c by the mitochondrial channel VDAC. Nature 1999; 399:483–7.
35. Saito M, Korsmeyer SJ, Schlesinger PH. BAX-dependent transport of cytochrome c reconstituted in pure liposomes. Nat Cell Biol 2000; 2:553–5.
36. Ghosh SP, Kulkarni S, Perkins MW, Hieber K, Pessu RL, Gambles K, et al. Amelioration of radiation-induced hematopoietic and gastrointestinal damage by Ex-RAD(R) in mice. J Radiat Res 2012; 53:526–36.
37. Zhang Y, Zhang X, Rabbani ZN, Jackson IL, Vujaskovic Z. Oxidative stress mediates radiation lung injury by inducing apoptosis. Int J Radiat Oncol Biol Phys 2012; 83:740–8.
38. Tessner TG, Muhale F, Riehl TE, Anant S, Stenson WF. Prostaglandin E2 reduces radiation-induced epithelial apoptosis through a mechanism involving AKT activation and bax translocation. J Clin Invest 2004; 114:1676–85.
39. Lee CL, Moding EJ, Cuneo KC, Li Y, Sullivan JM, Mao L, et al. p53 functions in endothelial cells to prevent radiation-induced myocardial injury in mice. Sci Signal 2012; 5:ra52.
40. Shimizu S, Narita M, Tsujimoto Y. Bcl-2 family proteins regulate the release of apoptogenic cytochrome c by the mitochondrial channel VDAC. Nature 1999; 399:483–7.
41. Elrod JW, Wong R, Mishra S, Vagnozzi RJ, Sakthievel B, Goonasekera SA, et al. Cyclophilin D controls mitochondrial pore-dependent Ca(2+) exchange, metabolic flexibility, and propensity for heart failure in mice. J Clin Invest 2010; 120:3680–7.
42. Halestrap AP, Clarke SJ, Javadov SA. Mitochondrial permeability transition pore opening during myocardial reperfusion–a target for cardioprotection. Cardiovasc Res 2004; 61:372–85.
43. Zamzami N, Kroemer G. The mitochondrion in apoptosis: how Pandora's box opens. Nat Rev Mol Cell Biol 2001; 2:67–71.
44. Di Lisa F, Carpi A, Giorgio V, Bernardi P. The mitochondrial

permeability transition pore and cyclophilin D in cardioprotection. Biochim Biophys Acta 2011; 1813:1316–22.

45. Murphy E, Steenbergen C. Mechanisms underlying acute protection from cardiac ischemia-reperfusion injury. Physiol Rev 2008; 88:581–609.

46. Weiss JN, Korge P, Honda HM, Ping P. Role of the mitochondrial permeability transition in myocardial disease. Circ Res 2003; 93:292–301.

47. Hunter DR, Haworth RA, Southard JH. Relationship between configuration, function, and permeability in calcium-treated mitochondria. J Biol Chem 1976; 251:5069–77.

48. Ngoh GA, Watson LJ, Facundo HT, Jones SP. Augmented O-GlcNAc signaling attenuates oxidative stress and calcium overload in cardiomyocytes. Amino Acids 2011; 40:895–911.

49. Assaly R, de TA, Paradis S, Jacquin S, Berdeaux A, Morin D. Oxidative stress, mitochondrial permeability transition pore opening and cell death during hypoxia-reoxygenation in adult cardiomyocytes. Eur J Pharmacol 2012; 675:6–14.

50. Di LF, Bernardi P. Mitochondrial function as a determinant of recovery or death in cell response to injury. Mol Cell Biochem 1998; 184:379–91.

51. Leach JK, Van TG, Lin PS, Schmidt-Ullrich R, Mikkelsen RB. Ionizing radiation-induced, mitochondria-dependent generation of reactive oxygen/nitrogen. Cancer Res 2001; 61:3894–01.

52. Limoli CL, Giedzinski E, Morgan WF, Swarts SG, Jones GD, Hyun W. Persistent oxidative stress in chromosomally unstable cells. Cancer Res 2003; 63:3107–11.

53. Mancini M, Anderson BO, Caldwell E, Sedghinasab M, Paty PB, Hockenbery DM. Mitochondrial proliferation and paradoxical membrane depolarization during terminal differentiation and apoptosis in a human colon carcinoma cell line. J Cell Biol 1997; 138:449–69.

54. Spodnik JH, Wozniak M, Budzko D, Teranishi MA, Karbowski M, Nishizawa Y, et al. Mechanism of leflunomide-induced proliferation of mitochondria in mammalian cells. Mitochondrion 2002; 2:163–79.

55. Franken NA, Hollaar L, Bosker FJ, Van Ravels FJ, van der Laarse A, Wondergem J. Effects of in vivo heart irradiation on myocardial energy metabolism in rats. Radiat Res 1993; 134:79–85.

56. Balietti M, Fattoretti P, Giorgetti B, Casoli T, Di SG, Solazzi M, et al. A ketogenic diet increases succinic dehydrogenase activity in aging cardiomyocytes. Ann N Y Acad Sci 2009; 1171:377–84.

57. Drose S. Differential effects of complex II on mitochondrial ROS production and their relation to cardioprotective pre- and postconditioning. Biochim Biophys Acta 2013; 1827:578–87.

58. Rustin P, Munnich A, Rotig A. Succinate dehydrogenase and human diseases: new insights into a well-known enzyme. Eur J Hum Genet 2002; 10:289–91.